

Nb lateral Josephson junctions induced by a NiFe cross strip

L. K. Lin, S. Y. Huang, J. H. Huang, and S. F. Lee

Citation: [Applied Physics Letters](#) **101**, 242601 (2012); doi: 10.1063/1.4770302

View online: <http://dx.doi.org/10.1063/1.4770302>

View Table of Contents: <http://scitation.aip.org/content/aip/journal/apl/101/24?ver=pdfcov>

Published by the [AIP Publishing](#)



FREE Multiphysics Simulation e-Magazine

DOWNLOAD TODAY >>

 **COMSOL**

Nb lateral Josephson junctions induced by a NiFe cross strip

L. K. Lin,^{1,2} S. Y. Huang,¹ J. H. Huang,² and S. F. Lee^{1,a)}

¹*Institute of Physics, Academia Sinica, Taipei 115, Taiwan*

²*Department of Materials Science and Engineering, National Tsing Hua University, HsinChu 300, Taiwan*

(Received 12 October 2012; accepted 21 November 2012; published online 10 December 2012)

We fabricated lateral junctions by crossing superconducting Nb strips in metallic contact with a ferromagnetic NiFe strip. Transport measurements on the Nb lateral junctions exhibit modulations of the critical current with a varying perpendicular magnetic field similar to a Fraunhofer interference pattern, which demonstrates the dc Josephson effect. The modulations of the critical current could be attributed to an effective weak link embedded in the Nb strip and formed a Josephson junction. Appearance of Shapiro steps on the current-voltage curves of these junctions when microwaves irradiation is applied proves the ac Josephson effect. The underlying physics of the effective weak link induced by the NiFe strip is discussed. © 2012 American Institute of Physics. [<http://dx.doi.org/10.1063/1.4770302>]

The heterogeneous properties around the interface between ferromagnet (F) and conventional s-wave superconductor (S) hybrid structures exhibit several remarkable phenomena. The Cooper pairs from the S can penetrate a short distance, $\xi_F = \sqrt{\hbar D_F / h_{ex}}$, into the F in the dirty limit, where D_F is the diffusion coefficient and h_{ex} is the magnetic exchange field in F, is one example of the proximity effect.¹ The ξ_F is only few nanometers due to the strong magnetic exchange field. Even in weak ferromagnets, it is only about 10 nm.² An S/F/S Josephson junction due to the proximity effect is characterized by phase coherent transfer of the Cooper pairs across the ferromagnet weak link between two superconducting electrodes. The oscillations of the pair correlations lead to alternating 0 and π junction in S/F/S devices, which have been observed in several experiments using strong and weak ferromagnet.^{3–5} Though the S/F proximity effect has attracted much attention, the inverse proximity effect, in which the ferromagnetic order-parameter penetrates into the superconductor, has rarely been reported experimentally. According to the quasiclassical approach,^{6–11} there are two possible profiles as “screening” and “antiscreening” for the induced magnetic moment inside the S. Whether the direction of the induced magnetic moment inside the S is antiparallel or parallel to the magnetization of F is correlative to the screening or antiscreening profiles. So far, only a few experimental observations of the inverse proximity effect were given by techniques like nuclear magnetic resonance,¹² neutron reflectometry,¹³ and Sagnac magnetometer,¹⁴ which gives accurately the spatial distribution of magnetic moments and provides the spin screening effect. Stamopoulos *et al.*¹⁵ suggest that the results of the magnetization measurement on the LaCaMnO/Nb hybrids can be attributed to the spin antiscreening. Recently, the evidence for induced magnetization in S/F heterostructures have been reported by the scanning tunneling spectroscopy study on YBaCuO/SrRuO₂¹⁶ and by electronic transport measurement in lateral double Josephson junction of Nb/PdFe.¹⁷ In this article, we present experimental observations of the dc and ac Josephson effects in

NiFe/Nb cross-strip samples. We argue that the effective weak link of the Josephson junction was induced by the inverse proximity effect around the Nb interface in contact with the strong ferromagnetic NiFe.

The samples were fabricated by electron beam lithography and the lift-off technique. NiFe strips 50 nm thick with 3 nm Au protective layer were deposited by dc magnetron sputtering onto Si substrates coated with SiO₂ first. After defining the cross bridge shape, Ar-ion etching was applied to remove the Au protective layer on the film surface immediately prior to the *in situ* 100 nm thick Nb deposition. The width of the NiFe strip was 0.7 μm , and the width of the Nb bridges were fixed at 1.5 μm . The image of one sample and measurement layout is given in the inset of Fig. 1(a). The transport properties were measured under various temperatures and magnetic fields, which were perpendicular to the film plane.

Our samples consist of a Nb strip and a cross NiFe strip. In Fig. 1(a), the resistance versus temperature curve shows a transition from the normal state with 15.2 Ω to the S state below the critical temperature $T_C = 6.0$ K. Fig. 1(b) shows the I-V curves, measured from 2 to 5 K, representing the current induced transitions to the normal state with critical current I_C defined by the onset of 1 μV . When out-of-plane magnetic fields were applied, the junctions exhibited a modulation of the I_C similar to the Fraunhofer interference pattern. Typical curves measured between 2 and 5 K for the sample in Fig. 1 are shown in Fig. 2. We can see that the periodicity of our data agree well with the function $I_0 |[\sin(\pi H / H_0)] / (\pi H / H_0)|$, which is drawn as a solid line in Fig. 2(a). Our data seem to show a slightly varying background superimposed on this curve. Estimating the crossed area between Nb and NiFe, we find the expected magnetic field that corresponds to one magnetic flux quantum through the area should be 19.7 Oe. The measured periodicity ΔH is approximately 23 Oe. The Fraunhofer interference pattern can be obtained at different temperature below T_C as shown in Fig. 2(b). The same numbers of periodic peaks can be observed. The amplitudes of I_C peaks reasonably decreased with increasing temperature.

^{a)}E-mail: leesf@phys.sinica.edu.tw.

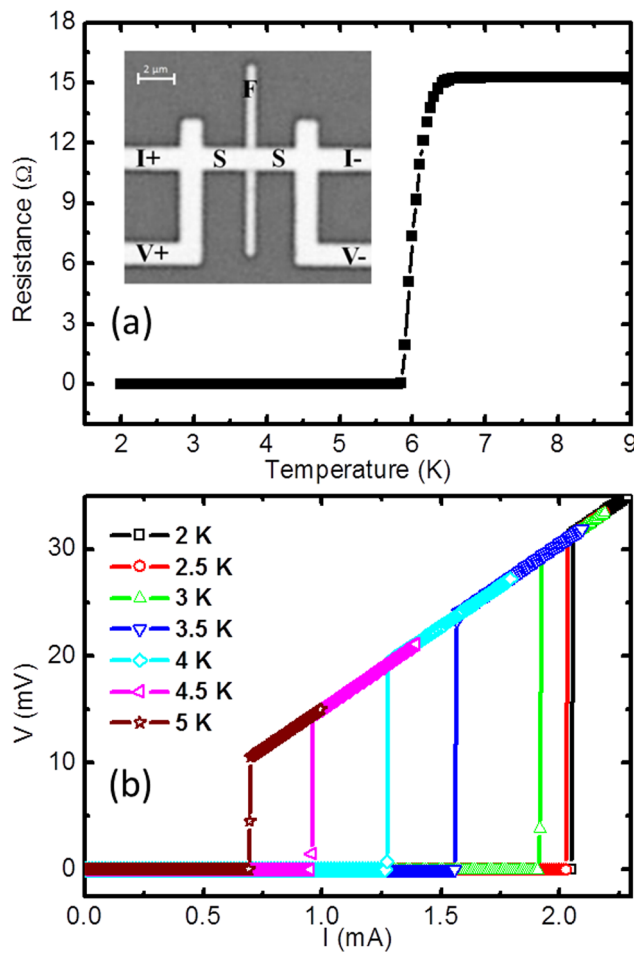


FIG. 1. (a) The resistance versus temperature curve of a $0.7\ \mu\text{m}$ wide NiFe junction. Inset shows the sample image and measurement layout. (b) Current versus voltage characteristics measured for the same junction at zero magnetic field and varying temperatures from 2 to 5 K which critical current I_C 's are defined.

The contribution of stray field and vortex pinning effects to our data should be considered. The NiFe is in long strip geometry. Due to the magnetic anisotropy, the magnetizations of NiFe prefer aligning along the in-plane long axis. The Fraunhofer interference pattern were measured under the out-of-plane field between ± 200 Oe. Such field is too small to rotate the magnetizations to the out-of-plane direction. We also checked the magnetization configurations of NiFe strip by the micro-magnetism simulation software OOMMF. There is no vertical stray field in the horizontal plane at the middle of the NiFe. The Nb strip is far from the ends of the $4\ \mu\text{m}$ long NiFe strip as shown in the inset of Fig. 1, the horizontal stray field from the ends of NiFe strip is quite small and Nb has high critical field, H_{C2} . Therefore, the stray field effect could be ruled out.

The critical current modulations might also result from vortex pinning effect in superconducting mixed state. Observations of the I_C modulations by vortex pinning effect in samples with designed artificial pinning sites were measured at the temperature very close to T_C ,^{18,19} i.e., in the superconducting mixed state. In our samples, there are no artificial pinning sites and the I_C modulations could be observed at all temperature between 2 K and T_C rather than only at very close to T_C . The behavior is very different to the vortex pinning effect. In

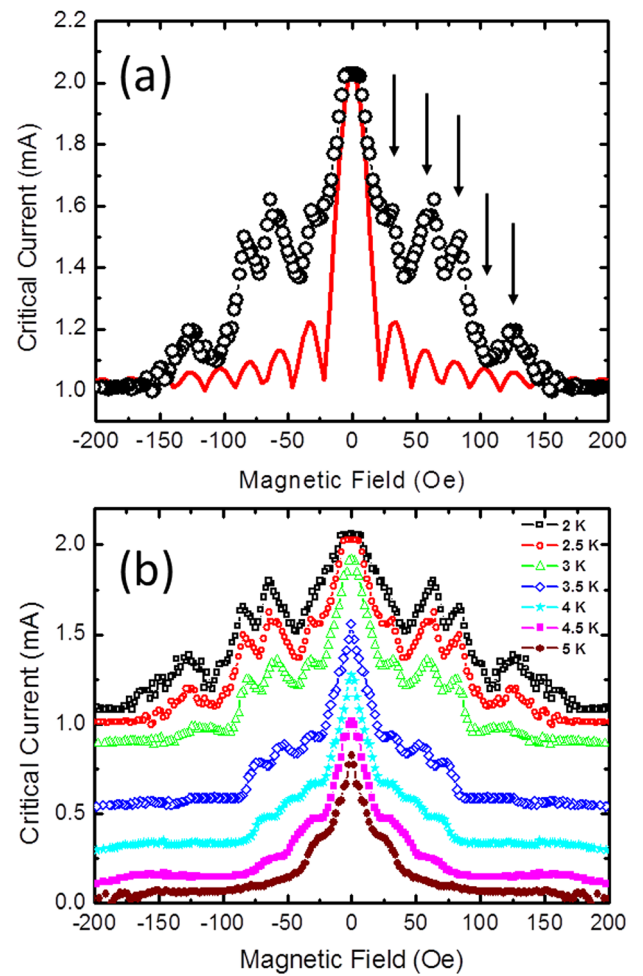


FIG. 2. (a) The periodic modulation of the critical current of the $0.7\ \mu\text{m}$ wide NiFe junction in a perpendicular magnetic field at 2.5 K similar to a Fraunhofer interference pattern. The red solid line is described by $I_0|\sin(\pi H/H_0)|/(\pi H/H_0)$ and is a guide to the eye. The arrows point to the peaks position. (b) The modulation of the critical current in a perpendicular magnetic field at varying temperatures from 2 to 5 K.

order to rule out the possibility of vortex pinning by defects and magnetic impurities, we checked Nb with crossed Cu instead of NiFe strips fabricated by the same condition and did not see any I_C modulations with magnetic field. Hence, the modulations of I_C demonstrate the dc Josephson effect.

To explain our data, we treat the Nb strip as an S- S_F -S junction such that the Josephson effect manifest itself as I_C oscillation on top of the I_C of the Nb strip background. The " S_F " denotes the effective weak link region embedded in Nb strip induced by the inverse proximity effect, where the net magnetic moments and superconductivity coexist in Nb. The S_F did not turn into a normal ferromagnet as indicated by the zero resistance as seen in Fig. 1(a) at low temperature. When the inverse proximity effect occurs, the penetration length of the induced magnetic moment in S should be a few coherence length ξ_S deep from the S/F interface as the theoretical prediction. However, when the magnetic moment was induced inside S in close vicinity to the S/F interface, a spin imbalanced population of electrons is formed. It is expected to lose its polarization at a distance comparable to the spin diffusion length. If the spin diffusion length is larger than the coherence length ξ_S , one would expect that the distances of the imbalance of the spin population would extend larger

than ξ_S . There are two different ways in the literature to determine the spin diffusion length. In current-perpendicular-to-plane (CPP) spin-valve structures, the spin diffusion length in Nb is estimated to be 25 and 48 nm.^{20,21} The other way is the non-local measurements by lateral spin diffusion.^{22,23} In the lateral dimension, the spins can travel through several hundred nanometers.^{24,25} The coherence length ξ_S of Nb is estimated around 10 nm, which is much shorter than the spin diffusion length mentioned above. Therefore, the embedded depth of S_F in Nb is expected to be larger than the coherence length ξ_S . The induced magnetization length in S larger than ξ_S was also observed by scanning tunneling spectroscopy study on YBaCuO/SrRuO.¹⁶

The zero resistance below T_C suggests a fully developed S state in the effective weak link S_F embedded in our Nb strip in contact with the NiFe strip. The Cooper pair wavefunctions in the effective weak link S_F is not diminished as in usual Josephson junctions. The single step during both temperature and current induced transitions suggests the superconductivity of the S_F region behaves as a whole with the neighboring Nb. Therefore, when the applied current reaches the critical value, the whole Nb strip turns to normal state. For comparison, we also fabricated samples without S_F region, Nb strips without NiFe strip. The I_C 's were much larger and no modulation behaviors could be observed. Thus, the I_C modulation we observed is associated with the S- S_F -S junction.

Vavra *et al.*¹⁷ studied lateral double junction of Nb and weak ferromagnetic Pd_{0.95}Fe_{0.05}. They observed Josephson junction behaviors only when temperature was close to T_C . It was attributed to that the S condensate in the adjacent Nb dominated over the inverse proximity effect at low temperature. In our case, the NiFe was used to induce the effective weak link in Nb. The inverse proximity effect induced by a strong F can be expected to survive at lower temperatures. The Fraunhofer interference patterns are clearly observed down to 2 K.

The phenomena of Josephson junctions should be confirmed by both dc and ac Josephson effects. When a Josephson junction is subject to an electro-magnetic radiation with frequency f_{rf} , the response of the supercurrent gives rise to the Shapiro steps in the dc current-voltage curve at voltages $V_n = nhf_{rf}/2e$, where n is an integer and h is the Planck's constant. We have irradiated our samples with a microwave source with frequencies from 5 to 15 GHz and fixed power of 13 dBm. The ac excitation Shapiro steps under different frequencies were observed on the dc I-V characteristics as shown in Fig. 3(a). The dc I-V curve at 5 GHz shows the steps at integer multiples of the Shapiro voltage. At 7 to 15 GHz, the I-V curves show the first integer Shapiro voltages, V_1 . The V_1 versus microwave frequency f_{rf} is plotted in Fig. 3(b). The voltage steps increase linearly with increasing microwave frequency. The solid line is described by $f_{rf}/V_{Sh} = 2e/h = 0.483 \text{ GHz}/\mu\text{V}$. Our experimental data agree well with the theoretical description. The Shapiro steps observation proves the ac Josephson effect in our samples. From the Fraunhofer patterns and the Shapiro steps measurements, the Josephson effect exists in our Nb strip crossed with the NiFe. The fact that the Josephson effect could be measured in the Nb strip suggests the weak link S_F possesses

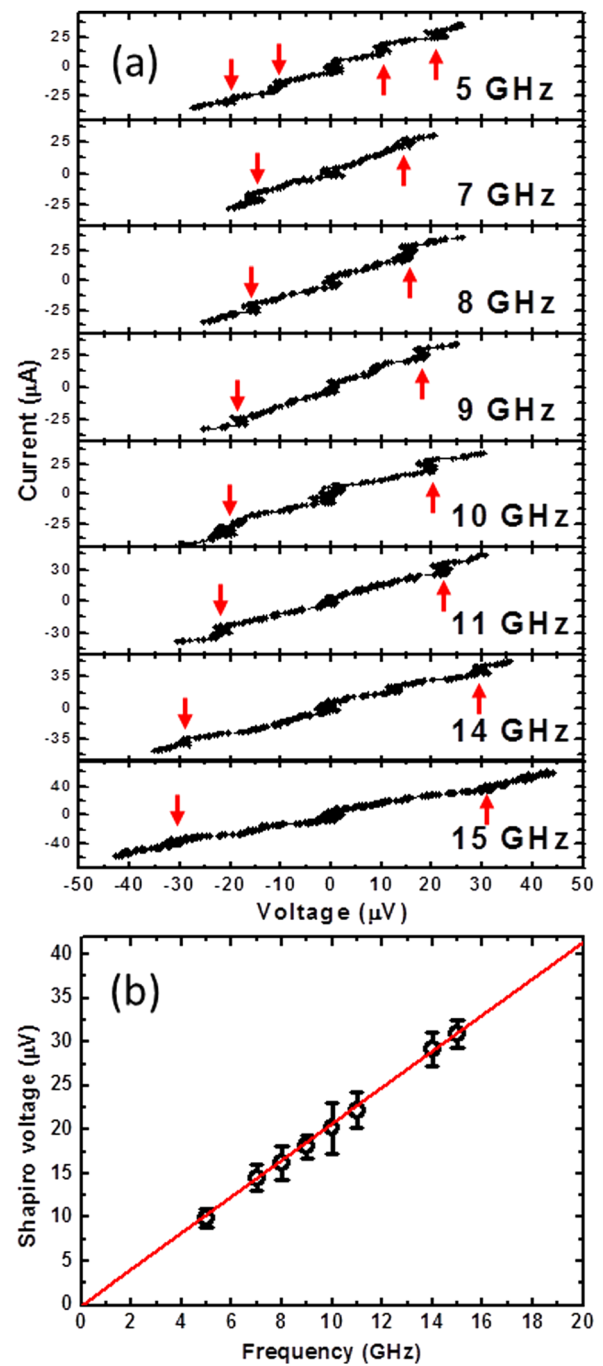


FIG. 3. (a) The Shapiro steps in the dc I-V characteristics under the irradiation microwaves with the frequencies varied from 5 to 15 GHz. (b) The Shapiro voltage and microwave frequency dependence. The red line is described by $f_{rf}/V_n = 2e/h = 483 \text{ MHz}/\mu\text{V}$.

a net magnetic moment induced by the contacting NiFe strip, i.e., an inverse proximity effect is taking place.

According to transport theory in a diffusive limit, I_C for a long S-N-S junction is proportional to $T^{3/2} \exp(\sqrt{(2\pi k_B T)/E_{Th}})$,²⁶ with the Thouless energy E_{Th} given by $\hbar D/L^2$, where D the diffusion constant of the normal (N) metal, and L the junction length. Though this may not apply to our case when there are the spin-polarized carriers in Nb, we try to analyze our data with the above relation. From the measured periodicity, $\Delta H = 23 \text{ Oe}$ of the Fraunhofer pattern of the $0.7 \mu\text{m}$ wide NiFe junction, the effective junction length $L = 0.58 \mu\text{m}$ can be estimated by $L = \Phi_0/W\Delta H$,

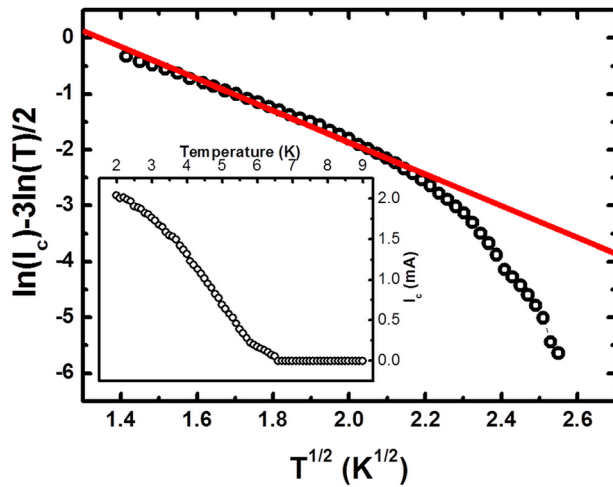


FIG. 4. Plotting $\ln(I_c) - 3\ln(T)/2$ versus \sqrt{T} with the red solid line corresponding to $E_{Th} = 66.6 \mu\text{eV}$. The inset shows the critical current versus temperature for the $0.7 \mu\text{m}$ wide NiFe junction.

where Φ_0 is the flux quantum ($20.7 \text{ Oe} \cdot \mu\text{m}^2$) and W is the width of the Nb bridge ($1.5 \mu\text{m}$). The E_{Th} are 42.9 and $29.4 \mu\text{eV}$ corresponding to $L = 0.58$ (effective junction length) and $0.7 \mu\text{m}$ (actual NiFe width) with $D = 2.19 \times 10^{-2} \text{ m}^2/\text{s}$. The inset in Fig. 4 shows the temperature (T) dependence of I_c . In Fig. 4, we plotted $\ln(I_c) - 3\ln(T)/2$ versus \sqrt{T} . The red solid line with E_{Th} of $66.6 \mu\text{eV}$ shows that the relation holds well at low temperatures. The E_{Th} calculated by the effective junction length underestimated the value when compared to the fitted value from the low temperature data. In our case, the weak link is embedded in the Nb strip and induced by the inverse proximity effect. In addition to the temperature pair-breaking effect, there should be a spin polarized carrier effect in Nb similar to the consequence of exchange field in NiFe. The above expression $I_c \propto T^{3/2} \exp(\sqrt{(2\pi k_B T)/E_{Th}})$ needs to be modified accordingly. Most of metallic weak links are realized within the diffusion regime and belong typically to a long junction limit which holds for $\Delta \gg E_{Th}$. For all our samples, the Thouless energy should be significantly smaller than the superconducting gap Δ of Nb. The relative strength between temperature and spin polarized carrier effects will be an interesting topic to pursue.

We have prepared Nb/NiFe cross geometry samples to create lateral Josephson junctions. The modulations of the critical current in a perpendicular magnetic field similar to the Fraunhofer interference pattern were observed, which demonstrates the dc Josephson effect. The Josephson effect could be observed at all temperature ranges investigation,

which indicates that the weak link region induced by NiFe is robust for Nb superconductivity. We also observed the ac Josephson effects by Shapiro steps measurement. The dc and ac Josephson effect observations prove the weak link of the Josephson junction was induced by the ferromagnetic NiFe, where the inverse proximity effect takes place.

The financial supports of the Academia Sinica and the National Science Council of Taiwan, Republic of China are gratefully acknowledged.

- ¹A. I. Buzdin, *Rev. Mod. Phys.* **77**, 935 (2005).
- ²S. Y. Huang, J. J. Liang, S. Y. Hsu, L. K. Lin, T. C. Tsai, and S. F. Lee, *Eur. Phys. J. B* **79**, 153 (2011).
- ³V. V. Ryazanov, V. A. Oboznov, A. Yu. Rusanov, A. V. Veretennikov, A. A. Golubov, and J. Aarts, *Phys. Rev. Lett.* **86**, 2427 (2001).
- ⁴H. Sellier, C. Baraduc, F. Lefloch, and R. Calemczuk, *Phys. Rev. B* **68**, 054531 (2003).
- ⁵J. W. A. Robinson, S. Piano, G. Burnell, C. Bell, and M. G. Blamire, *Phys. Rev. Lett.* **97**, 177003 (2006).
- ⁶F. S. Bergeret, A. F. Volkov, and K. B. Efetov, *Europhys. Lett.* **66**, 111 (2004).
- ⁷F. S. Bergeret and N. Garcia, *Phys. Rev. B* **70**, 052507 (2004).
- ⁸V. N. Krivoruchko and E. A. Koshina, *Phys. Rev. B* **66**, 014521 (2002).
- ⁹F. S. Bergeret, A. F. Volkov, and K. B. Efetov, *Phys. Rev. B* **69**, 174504 (2004).
- ¹⁰F. S. Bergeret, A. Levy Yeyati, and A. Martin-Rodero, *Phys. Rev. B* **72**, 064524 (2005).
- ¹¹M. Yu. Kharitonov, A. F. Volkov, and K. B. Efetov, *Phys. Rev. B* **73**, 054511 (2006).
- ¹²R. I. Salikhov, I. A. Garifullin, N. N. Garifyanov, L. R. Tagirov, K. Theis-Brohl, K. Westerholt, and H. Zabel, *Phys. Rev. Lett.* **102**, 087003 (2009).
- ¹³J. Stahn, J. Chakhalian, Ch. Niedermayer, J. Hoppler, T. Gutberlet, J. Voigt, F. Treubel, H.-U. Habermeyer, G. Cristiani, B. Keimer, and C. Bernhard, *Phys. Rev. B* **71**, 140509 (2005).
- ¹⁴J. Xia, V. Shelukhin, M. Karpovskii, A. Kapitulnik, and A. Palevski, *Phys. Rev. Lett.* **102**, 087004 (2009).
- ¹⁵D. Stamopoulos, N. Moutis, M. Pissas, and D. Niarchos, *Phys. Rev. B* **72**, 212514 (2005).
- ¹⁶I. Asulin, O. Yuli, G. Koren, and O. Millo, *Phys. Rev. B* **79**, 174524 (2009).
- ¹⁷O. Vavra, W. Pfaff, and Ch. Strunk, *Appl. Phys. Lett.* **95**, 062501 (2009).
- ¹⁸Lance Horng, J. C. Wu, T. C. Wu, and S. F. Lee, *J. Appl. Phys.* **91**, 8510 (2002).
- ¹⁹M. Velez, J. I. Martin, J. E. Villegas, A. Hoffmann, E. M. Gonzalez, J. L. Vicent, and I. K. Schuller, *J. Magn. Magn. Mater.* **320**, 2547 (2008).
- ²⁰W. Park, D. V. Baxter, S. Steenwyk, I. Moraru, W. P. Pratt, Jr., and J. Bass, *Phys. Rev. B* **62**, 1178 (2000).
- ²¹J. Y. Gu, J. A. Caballero, R. D. Slater, R. Loloe, and W. P. Pratt, Jr., *Phys. Rev. B* **66**, 140507 (2002).
- ²²S. Takahashi and S. Maekawa, *J. Phys. Soc. Jpn.* **77**, 031009 (2008).
- ²³N. Poli, J. P. Morten, M. Urech, A. Brataas, D. B. Haviland, and V. Korenivski, *Phys. Rev. Lett.* **100**, 136601 (2008).
- ²⁴J. Bass and W. P. Pratt, Jr., *J. Phys.: Condens. Matter* **19**, 183201 (2007).
- ²⁵L. K. Lin, S. Y. Huang, J. K. Lin, J. H. Huang, and S. F. Lee, *J. Appl. Phys.* **109**, 07E155 (2011).
- ²⁶M. S. Anwar, F. Czeschka, M. Hesselberth, M. Porcu, and J. Aarts, *Phys. Rev. B* **82**, 100501 (2010).